RevMexAA (Serie de Conferencias), **25**, 50–52 (2006)

BENEFITS OF IMAGE DECONVOLUTION IN CCD IMAGERY

O. Fors,[1,2] M. Merino,[1] X. Otazu,[3] R. Cardinal,[4] J. Núñez,[1,2] and A. Hildebrand[4]

RESUMEN

En este trabajo mostramos, cómo la deconvolución basada en ondículas de imágenes obtenidas con telescopios de campo ancho, incrementa el límite de magnitud en $\Delta R\sim0.6$ y supone una mejora en la separación de imágenes. La precisión astrométrica no disminuye, lo cual hace que la técnica sea válida para proyectos astrométricos. Así mismo aplicamos el proceso de deconvolución a una serie de imágenes obtenidas con la repotenciada cámara Baker-Nunn del Observatorio Astrofísico de Rothney.

ABSTRACT

We show how wavelet-based image deconvolution can provide to wide-field CCD telescopes an increase in limiting magnitude of $\Delta R\sim0.6$ and significant deblending improvement. Astrometric accuracy is not distorted, therefore, the feasibility of the technique for astrometric projects is validated. We apply the deconvolution process to a set of images from the recently refurbished Baker-Nunn camera at Rothney Astrophysical Observatory.

Key Words: **METHODS: DATA ANALYSIS — TECHNIQUES: IMAGE PROCESSING**

1. INTRODUCTION

With the upcoming of the multiresolution concept based on wavelets, image deconvolution algorithms have improved their performance, overall in terms of noise amplification prevention (Starck et al. 2002). However, the use of this kind of techniques is still not wide-spread and is restricted to very specific applications. For instance, the scientific throughput of the *HST* and large ground-based telescopes, whose instrumental aspects are very well known (PSF, SNR), justifies the supplementary effort in data analysis. In this work, we apply a wavelet-based deconvolution algorithm to a more common situation, which is a wide-field CCD telescope dedicated to astrometric purposes.

2. ALGORITHM DESCRIPTION

A complete description of wavelet transform can be found at Mallat (1999). Among other properties, the wavelet transform decouples spatial and frequential contents and offers better noise vs signal discrimination than using a Fourier transform method. Since image deconvolution in presence of noise is an ill-posed inverse problem, and because most popular algorithms are non linear and iterative, the noise is amplified as mathematical convergence is reached. Thus, noise amplification prevention is a key feature for whatever deconvolution algorithm. The algorithm used belongs to the group based on a maximum likelihood estimator (MLE) derived by following a bayesian methodology. The algorithm incorporates the presence of Poisson (Lucy 1974) and Gaussian noise (Núñez & Llacer 1993). In a more recent upgrade (Otazu 2001), the multiresolution concept with wavelet decomposition was incorporated to the algorithm which, in addition, performs a selective deconvolution over areas of the image that exhibit different degrees of resolution and noise level. This procedure avoids large residuals and asymptotically stabilizes the solution with the number of iterations.

3. APPLICATION BAKER-NUNN DATA

We apply the deconvolution process to a set of 9 1Kx1K subframes of the same sky region taken with the Baker-Nunn camera at Rothney Astrophysical Observatory (Calgary, Canada). This instrument was recently (2004) refurbished as an equatorial camera for automatic CCD work. Optics have been upgraded with a field-flattener corrector lens, which provide an outstanding FOV of 4.2°x4.2° with high quality optical performance (spot size $\sim 20\mu m$). It is dedicated to NEOs detection in the northern portion of the sky. Its moderate undersampling ($3.9''$/pix) results in common object blending and the PSF to be slightly correlated with seeing. This is the methodology we follow:

[1]Departament d'Astronomia i Meteorologia, Universitat de Barcelona, Barcelona, Spain (ofors@am.ub.es).
[2]Observatori Fabra, Barcelona, Spain.
[3]Centre de Visió per Computador, Universitat Autònoma de Barcelona, Bellaterra, Spain.
[4]Department of Geology and Geophysics, University of Calgary, Canada.

1. CCD image calibration: bias, dark and flatfield correction,
2. the first image of the sequence (I_1) and the corresponding subset of the USNOA2.0 catalog (Monet et al. 1998) are taken as references. Astrometric plate transformations of every image with respect to I_1 and the catalog are computed,
3. aperture photometry of all the stars. A selection list of PSF candidates, excluding saturated and faintest ones, is carried out. This is done automatically and checked by the operator,
4. PSF fitting with the list created in (3). Different PSF models are considered: purely analytical (*Gaussian*, *Moffat* and *Lorentz*) and hybrid (*Penny*),
5. image deconvolution with computed flatfield and PSFs. The algorithm was executed with partial results up to 200 iterations.
6. object detection and matching with I_1 and catalog,
7. compute limiting magnitude gain with respect to USNO R magnitude,
8. compute internal astrometric error before and after deconvolution with all the common (x,y) positions in all 10 images. Detection was carried out with `sextractor` package (Bertin & Arnouts 1996) with a threshold of 3σ. The rest of steps were run inside `IRAF` (`ccdproc`, `daophot`, `imcoords`).

4. RESULTS

The convergence of the algorithm reached its asymptotic value at about 180 iterations in all the frames. In this order, *Penny*, *Lorentz* and *Moffat15* were the PSF models which best fit the original data, following the given sequence. However, in terms of new detections in the deconvolved data, the best performance was very closely for *Lorentz* and *Moffat15*. In Figure 1, we show new detections supplied by deconvolution due to SNR increase and resolution gain (note deblend of the central pair). A limiting magnitude gain of $\Delta R{\sim}0.6$ was derived from Figure 2. Finally, Figure 3 shows the residual maps for original and a deconvolved images. Their dispersions, assumed to be an estimate of the internal astrometric errors, were found to be $(\sigma_x,\sigma_y)=(0.0766, 0.0828)$ and $(0.0700, 0.0899)$ pixels, respectively. Therefore, we can conclude that deconvolution did not change σ significantly.

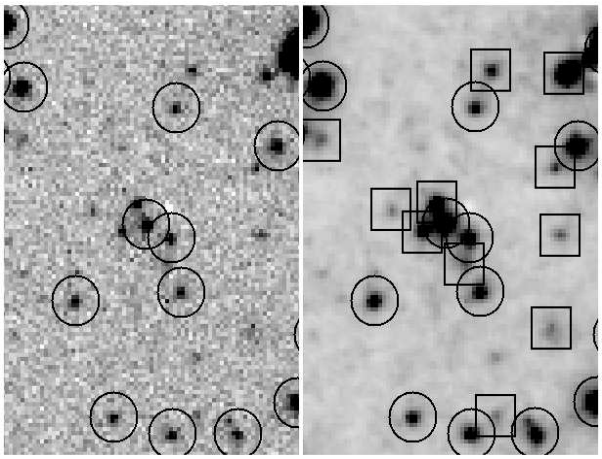

Fig. 1. Subset of detections in original image (left) and 60-iteration deconvolved image (right). Boxes indicate new detections. Note images are displayed with *zscale* LUT, which optimizes low values above background level.

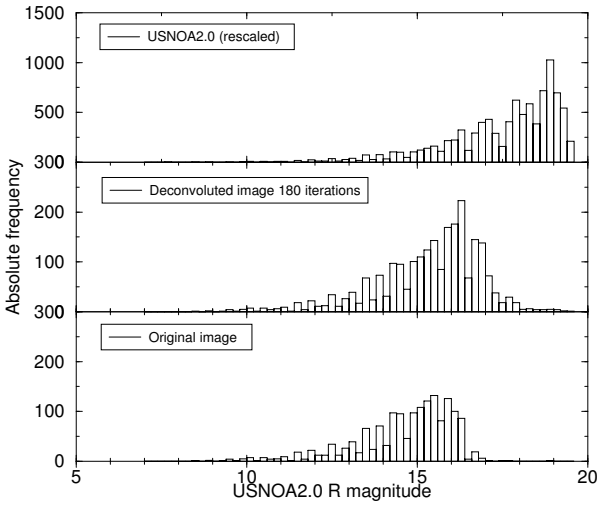

Fig. 2. Limiting magnitude gain.

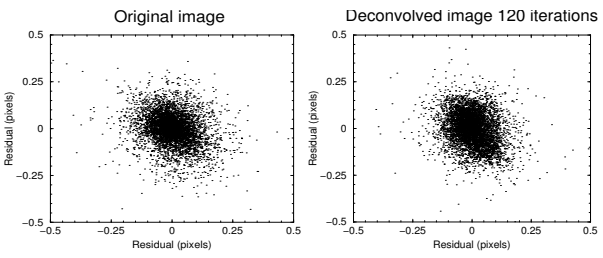

Fig. 3. Change in internal astrometric error.

5. CONCLUSIONS

We show that wavelet-based image deconvolution can provide, for wide-field CCD telescopes, an average increase in limiting magnitude of $\Delta R \sim 0.6$ and an improvement in resolution which contributes to deblending capabilities. Astrometric accuracy is not distorted during the process, therefore, the feasibility of the presented technique for astrometric projects is validated. Given the generic context of this work, our conclusions may be extrapolated to data from a large number of observational facilities.

REFERENCES

Bertin, E. & Arnouts, S. 1996, A&AS, 117, 393
Lucy, L. 1974, AJ, 79, 745
Mallat, S. 1999, A wavelet tour of signal processing 2nd edition, Academic Press, New York
Monet, D., et al. 1998, VizieR Online Data Catalog, 1252
Núñez, J. & Llacer, J. 1993, PASP, 105, 1192
Otazu, X. 2001, Ph. D. Thesis, University of Barcelona, Spain. http://www.tdx.cesca.es
Starck, J. L., Pantin, E., & Murtagh, F. 2002, PASP, 114, 1051